SEMARAK ILMU PUBLISHING

CFD Letters

Journal homepage:
https://semarakilmu.com.my/journals/index.php/CFD_Letters/index
ISSN: 2180-1363

Investigation of Sloshing in Different Tank Shapes using Smoothed Particle Hydrodynamics

Andi Trimulyono[1,*], Suci Utami[1], Deddy Chrismianto[1], Parlindungan Manik[1]

[1] Department of Naval Architecture, Faculty of Engineering, Universitas Diponegoro, Indonesia

ARTICLE INFO

Article history:
Received 15 May 2023
Received in revised form 12 June 2023
Accepted 10 July 2023
Available online 1 December 2023

Keywords:
Tank Shape; Sloshing; SPH; Dynamic Pressure; Hydrodynamic Force

ABSTRACT

Sloshing is the violent motion of a resonant fluid in a moving tank; when the fluid moves and interacts with the tank, the dynamic pressure from such an interaction can cause large fluid deformations with tank walls. In this study, a 3D numerical simulation of sloshing was carried out with five variations of the tank model, i.e., prismatic, rectangular, tube, spherical, and the new model tank with a filling ratio of 25% and 50%. Forced oscillation motion in a roll used frequencies 1.04 Hz and 1.34 Hz. The amplitude of movement was 8.66°. One pressure sensor was used to measure dynamic pressure in the mid of the tank. Because sloshing deals with large deformation and discontinuities, the particle method was suitable for the application. This study used smoothed particle hydrodynamics based on weakly compressible SPH (WCSPH). SPH is a Lagrangian meshless method known as mesh-free computational fluid dynamics. Open-source SPH solver DualSPHysics version 5.0 was used to reproduce sloshing in different tank shapes; in addition, advanced visualization was performed using the VisualSPHysics add-on in Blender version 2.92. The sloshing visualization is more realistic and attractive than conventional SPH post-processing. The results of this study indicate that different tank shapes influence reducing the value of dynamic pressure and hydrodynamic force. It is found that a practical tank shape is a tube tank and a new model tank with a reduced dynamic pressure value of 9% and 11% and a reduced hydrodynamic force value of 36% and 48%.

1. Introduction

Sloshing is a natural phenomenon of liquid carriers such as airplanes, ships, and trucks. Sloshing is the violent flow due to resonant fluid in a moving tank that could be caused by external force or forced resonant motion. When an energetic sloshing inside the tank, significant impact pressure could arise. As a result, structural damage in the wall of the tank could happen. Another reason is explosion would happen by sloshing when its fluid is volatile such as fuel carrier, LNG, and LPG. Recently a study of sloshing has been demanding as the results of liquid carriers have become larger compared with two decades ago. The LNG carrier is the most demanding sloshing analysis because the carrier has become more significant than a few years ago. Because sloshing deals with large

* *Corresponding author.*
E-mail address: anditrimulyono@live.undip.ac.id (Andi Trimulyono)

https://doi.org/10.37934/cfdl.15.12.1933

deformations and discontinuities of fluid movement, the particle method is one of the methods that are suitable to apply. One primary particle method is smoothed particle hydrodynamics (SPH), developed for astrophysical problems. Later on, Monaghan developed SPH for free surface flow with dam break and waves on the beach [1]. Moreover, the study improved the SPH for multi-phase problems [2]. The advantage of SPH attracts many researchers to widen SPH application not only for coastal and civil engineering problems.

The SPH application for sloshing was conducted for rectangular tanks in two and three dimensions with long-duration sloshing [3,4]. The study revealed that SPH well reproduced the sloshing phenomena regarding surface elevations and forces on the tank. Sloshing inside a ship's LNG fuel tank was conducted in 3 hours duration in real-time and could provide reasonable local pressure estimations [5]. Multi-phase flow sloshing was performed with δ-SPH and particle shifting technique [6], and a similar study was conducted with a prismatic tank for two and three dimensions of two-phase SPH [7,8]. The results showed SPH has good agreement with both quantitative and qualitative, though in three-dimension computation takes time to compare with mesh-based CFD solver. Sloshing in a rectangular tank with an elastic baffle was conducted using open-source SPH solver SPHinXsys [9], and a similar study was carried out with DualSPHysics for a rectangular tank [10,11]. Moreover, mesh based CFD solver for cryogenic fuel storage tank under external sloshing excitation performed with VOF method coupled with the mesh motion treatment [12-14]. CFD mesh based was widely used not only for sloshing, for example medicine, industrial and Marine engineering [15-18]. It showed that SPH is one of the major techniques for solving violent sloshing in tanks.

The aims of present study is verify the SPH's ability to analyze the sloshing phenomenon and identify the effect of tank shape on the sloshing phenomenon. The sloshing experiment was based on experimental works [19] with a 25% and 50% filling ratio. Four different tanks shape were used in this study, i.e., prismatic, rectangular, tube, spherical and new tank. Firstly, the pressure dynamic of the prismatic tank was validated based on experimental works. Later on, the exact position of the pressure gauge was used to measure dynamic pressure for other tank shapes. The filling ratio and width of the tank were kept the same.

Furthermore, a comparison of each simulated tank shape's hydrodynamic forces and free surface deformation was made. DualSPHysics version 5.0 [20,21] reproduces sloshing in different tank shapes. Moreover, advanced post-processing was carried out using VisualSPHysics, added in Blender [22]. There are many studies on sloshing, but only some studies have combined it with advanced post-processing. The results indicated SPH could reproduce dynamic pressure, and the effectiveness of the tank shape showed a minor impact on the sloshing phenomenon.

2. Methodology

2.1 Experimental Condition

Experimental condition of sloshing was based on Trimulyono *et al.,* [19] which a prismatic tank was used to reproduce sloshing in membrane type LNG carrier. There are three pressure sensor to capture dynamic pressure located in mid of tank, in this paper only one pressure sensor P1 was used to compare with SPH (see Figure 1). An external roll frequency excitation 1.04 Hz was used with amplitude of motion 8.66°, where height, width, length and water height of tank are 0.21, 0.30, 0.38, and 0.0525, respectively (see Table 1). The center of rotation is located in higher of tank as seen as showed in the Figure 1.

Table 1
Dimension of prismatic tank (units in meter)

Dimension	
Height (h)	0.21
Width (*l*)	0.30
Length (L)	0.36
Water height (d)	0.0525

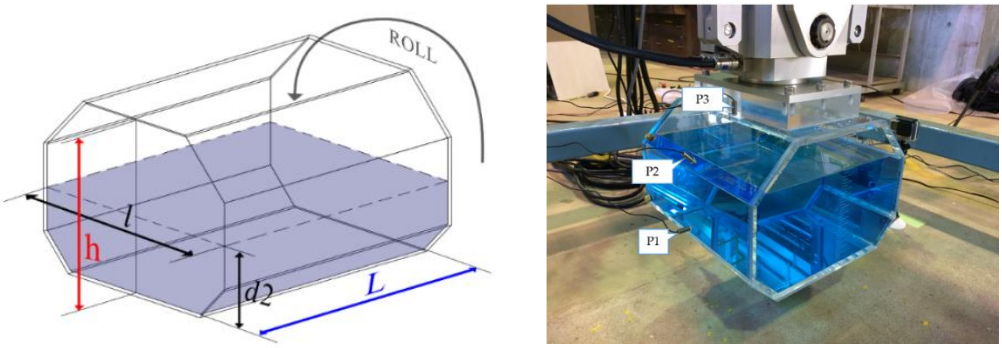

(a) (b)

Fig. 1. The sketch of (a) prismatic tank and (b) prismatic tank in experiment

2.2 Smoothed Particle Hydrodynamics (SPH)

SPH is one particle method developed for free surface by Monaghan and was later widely used for engineering problems. The SPH method discretized the computational domain into points or particles weighted by distance or smoothed length. To reduce the contribution, range from close particles, the quantities are calculated as a weighted sum from those particles within the smoothing length (*h*). The particle properties such as mass, velocity, and position are calculated with the weighting or kernel functions. The essential elements of the SPH technique, which is based on integral interpolants, are detailed in Ref. [23].

Figure 2 illustrates that particle *a* has distance r_{ab} with particle *b* with smoothing length (*h*) to calculate particle contribution in the kernel function W_{ab}. Eq. (1) showed the integral approximation field function *A(r)* in the domain (Ω). The particle approximation is shown in Eq. (2) as the sum of the neighboring particles with respect to the compact support of particle *a* at spatial point *r*. In this study, All simulations employed the Wendland kernel function, where α_D is equal to 21/164πh3 in 3D, and *q* is the nondimensional distance between particles *a* and *b* represented as *r/h* in Eq. (3). Eq. (4) is the continuity equation with the delta-SPH term to eliminate spurious pressure in SPH. The momentum equation in the SPH framework showed in Eq. (5), where **g** represents gravity acceleration, P_a and P_b are pressures in particles *a* and *b*. Π_{ab} is the artificial viscosity term, where $\mu_{ab} = h\boldsymbol{v}_{ab} \cdot \frac{\boldsymbol{r}_{ab}}{(\boldsymbol{r}_{ab}^2+\eta^2)}$, $\eta^2 = 0.01h^2$ $\bar{c}_{ab} = 0.5(c_a + c_b)$ is the mean speed of sound, and to achieve proper dissipation, the artificial viscosity coefficient must be adjusted. DualSPHysics is based on weakly compressible SPH (WCSPH), and an equation of state based is used in WCSPH shown in Eq. (6) where c_0, ρ_0, and γ are the speed of sound at the reference density, and polytrophic constant, respectively. Because of the stiffness of this equation, pressure could oscillate even with a slight change in density.

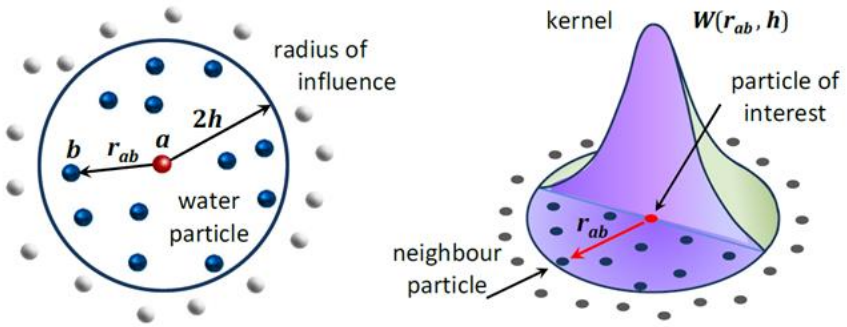

Fig. 2. Radius of the smoothing length and kernel function in SPH [18]

$$A(\boldsymbol{r}) = \int_{\Omega} A(\boldsymbol{r}) W(\boldsymbol{r} - \boldsymbol{r}', h)\, d\boldsymbol{r} \tag{1}$$

$$A(\boldsymbol{r}_a) \approx \sum_b A(\boldsymbol{r}_b) W(\boldsymbol{r}_a - \boldsymbol{r}_b, h) \frac{m_b}{\rho_b} \tag{2}$$

$$W(q) = \alpha_D \left(1 - \frac{q}{2}\right)^4 (2q + 1) \quad 0 \le q \le 2 \tag{3}$$

$$\frac{d\rho_a}{dt} = \sum_b m_b \boldsymbol{v}_{ab} \cdot \nabla_a W_{ab} + 2\delta_\Phi h c_0 \sum_b (\rho_{b-}\rho_a) \frac{\boldsymbol{r}_{ab} \cdot \nabla_a W_{ab}}{\boldsymbol{r}_{ab}^2} \frac{m_b}{\rho_b} \tag{4}$$

$$\frac{d\boldsymbol{v}_a}{dt} = -\sum_b m_b \left(\frac{P_{a+P_b}}{\rho_a \cdot \rho_b} + \Pi_{ab}\right) \nabla_a W_{ab} + \mathbf{g}$$

$$where\ \Pi_{ab} = \begin{cases} \dfrac{-\alpha \overline{c_{ab}} \mu_{ab}}{\overline{\rho_{ab}}} & \boldsymbol{v}_{ab} \cdot \boldsymbol{r}_{ab} < 0 \\ 0 & \boldsymbol{v}_{ab} \cdot \boldsymbol{r}_{ab} > 0 \end{cases} \tag{5}$$

$$P = \frac{c_0^2 \rho_0}{\gamma} \left[\left(\frac{\rho}{\rho_0}\right)^\gamma - 1\right] \tag{6}$$

Table 2 shows the computational setup for DualSPHysics code based on a previous study [10]. Coefound, Coefh, and CFL are the coefficient of sound, coefficient of smoothing length, and coefficient of Courant–Friedrichs–Lewy, respectively. The initial particle distance is 16 mm for two filling ratio conditions with a physical time is 28 seconds. a delta-SPH was used to reduce the spurious pressure field [24]. Figure 3 showed the displacement of the tank both for a filling ratio of 25% and 50%. The movement is forced oscillation based on a forced oscillation machine's four degrees of freedom (4DoF) based on experimental works [19]. Figure 4 illustrates the tank shape used for sloshing simulation with the same width of tank and filling ratios. There are four new tanks were used to reproduce sloshing with the same condition as sloshing in a prismatic tank. The width and filling ratio of the tank was the same in all tanks. Because the motion is regular and the pressure sensor location is in mid of the tank, the only motion is affected by the dynamic pressure. This is one of the reasons the width and filling ratio of the tank does not change, the other reason is a validation of dynamic pressure made based on the experimental of a prismatic tank. Figure 5 illustrates different shapes of fluid in particle (a), iso surface (b), and advanced rendering using Blender (c). It showed the advanced rendering post-processing made fluid in SPH seem realistic and similar to reality (see Figure 4. (d)).

Table 2
Parameter setup of the SPH computation

Parameters	
Kernel function	Wendland
Time step algorithm	Symplectic
Artificial viscosity coefficient (α)	0.01
Coefound	60
Particle spacing (mm)	16
Coefh	1.2
CFL	0.2
Delta-SPH (δϕ)	0.1
Simulation time (s)	28

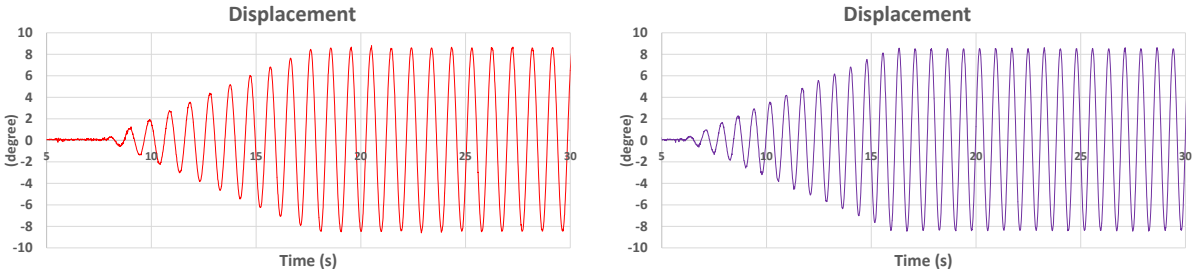

Fig. 3. The time history of tank displacement in rolling motion for filling ratio (a) 25% and (b) 50%

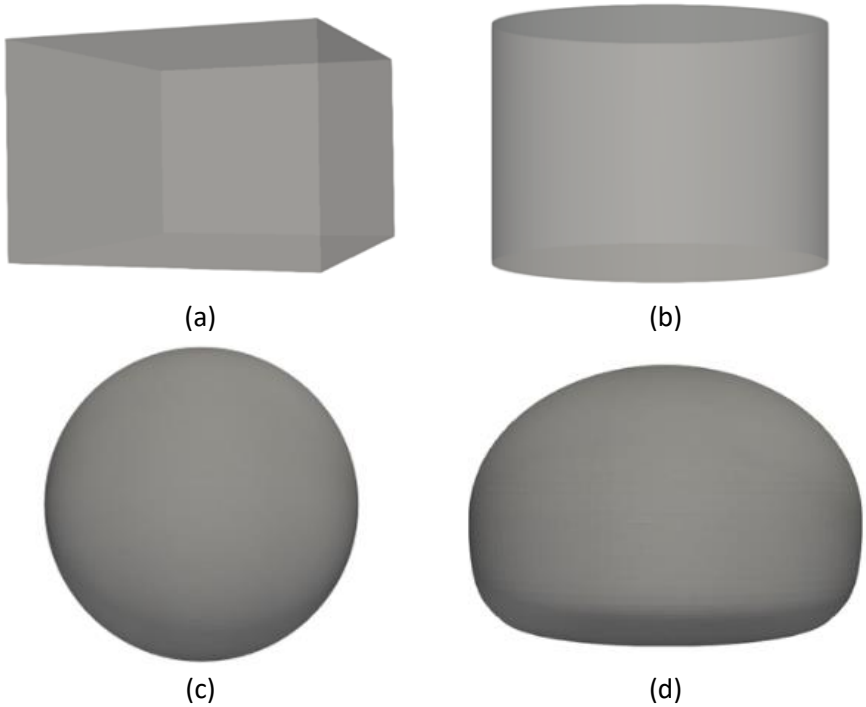

Fig. 4. Variations in tank shapes for sloshing simulation in (a) rectangular, (b) tube, (c) spherical, and (d) new tank design

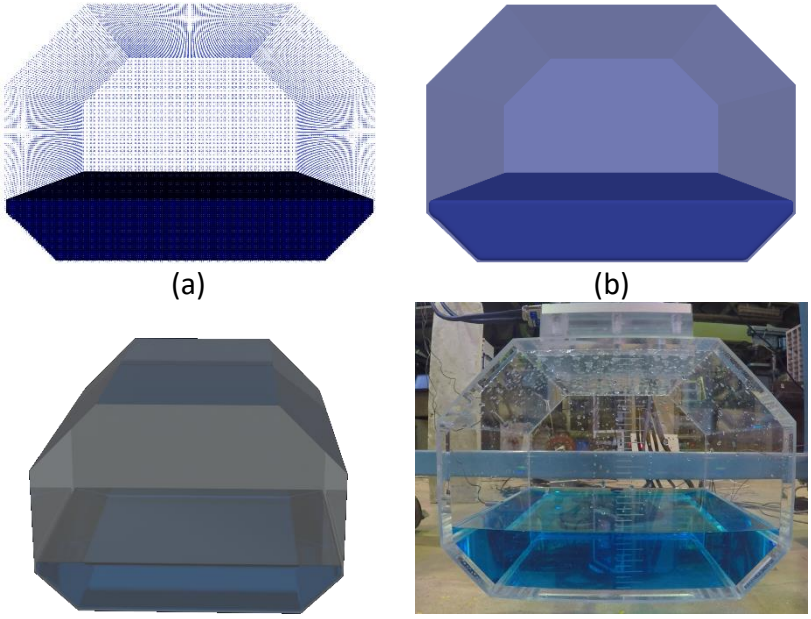

Fig. 5. Visualizations of the (a) particle, (b) iso-surface, (c) surface texture, and (d) experiment

3. Results

3.1 Dynamic Pressure

This section discusses the dynamic pressure of sloshing in each tank shape from the SPH result. Figure 6 and 7 illustrates dynamic pressure in the prismatic, rectangular, tube, spherical, and new model tank in the 25% and 50% filling ratio. The red and black are experimental and SPH, respectively. Figure 6 (a) showed a comparison of dynamic pressure between SPH with experiment results, it was found that was a spurious pressure though in this simulation delta-SPH was employed. In this simulation, we use Dynamic Boundary Condition (DBC) that when using DBC in SPH simulation, a gap between fluid particles and boundary particles occurs, caused by an artificial force exerted on the boundary particles [25]. It makes the point measurements by the pressure probe rather difficult to set on exact positions on the wall. Therefore, the gap between the boundary and fluid particles must be considered to contain the typical pressure probe. Moreover, the equation of state based on Tait's equations is very stiff. That small change in density creates a significant change in pressure which makes pressure fluctuate in WCSPH. In addition, the truncated kernel function decreases accuracy slightly because the pressure sensor is located near the free surface and on the edge of the tank. The latest version of DualSPHysics has a new function of Modified Dynamic Boundary Condition (MDBC) to vanish the gap between fluid and boundary particle and also reduce the pressure noise [26].

Figure 6 (b) and Figure 7 (b) shows a comparison of the dynamic pressure of prismatic, rectangular, and tube tank. The dynamic pressure tendency showed a similarity between prismatic tanks, although the volume of the tank is different. It can be explained because dynamic pressure is influenced by the speed of the fluid. There is a minor difference shown in spherical and new model tanks (see Figure 6 (c) and (d)). Figure 6 (c) and Figure 7 (c) shows a comparison of the dynamic pressure of prismatic, spherical, and new model tank. It was shown that the tube tank and new model tank are the most effective in reducing dynamic pressure compared to the other three tank shapes. The reduction is over 9% for the 25% filling ratio and 4% for the 50% filling ratio it can be seen in

Figures 8 (c) and (e) that water becomes slightly calmer and the impact pressure to the wall of the tank is lower.

Figure 7 showed dynamic pressure for a 50% filling ratio, the accuracy becomes slightly worse compared 25% filling ratio. The impact pressure could not produce by SPH only dynamic pressure caused by the motion of fluid could be reproduced. A similar trend appears in the filling ratio of 50% dynamic pressure shows similar magnitude for prismatic, rectangular, tube, spherical and new model tanks (see Figure 7 (b) and (c)). Figures 8 and 9 showed dynamic pressure for filling ratios of 25% and 50% in all tank shapes. It was found fluid particles showed noise in some parts, this is also one classical problem in the WCSPH scheme.

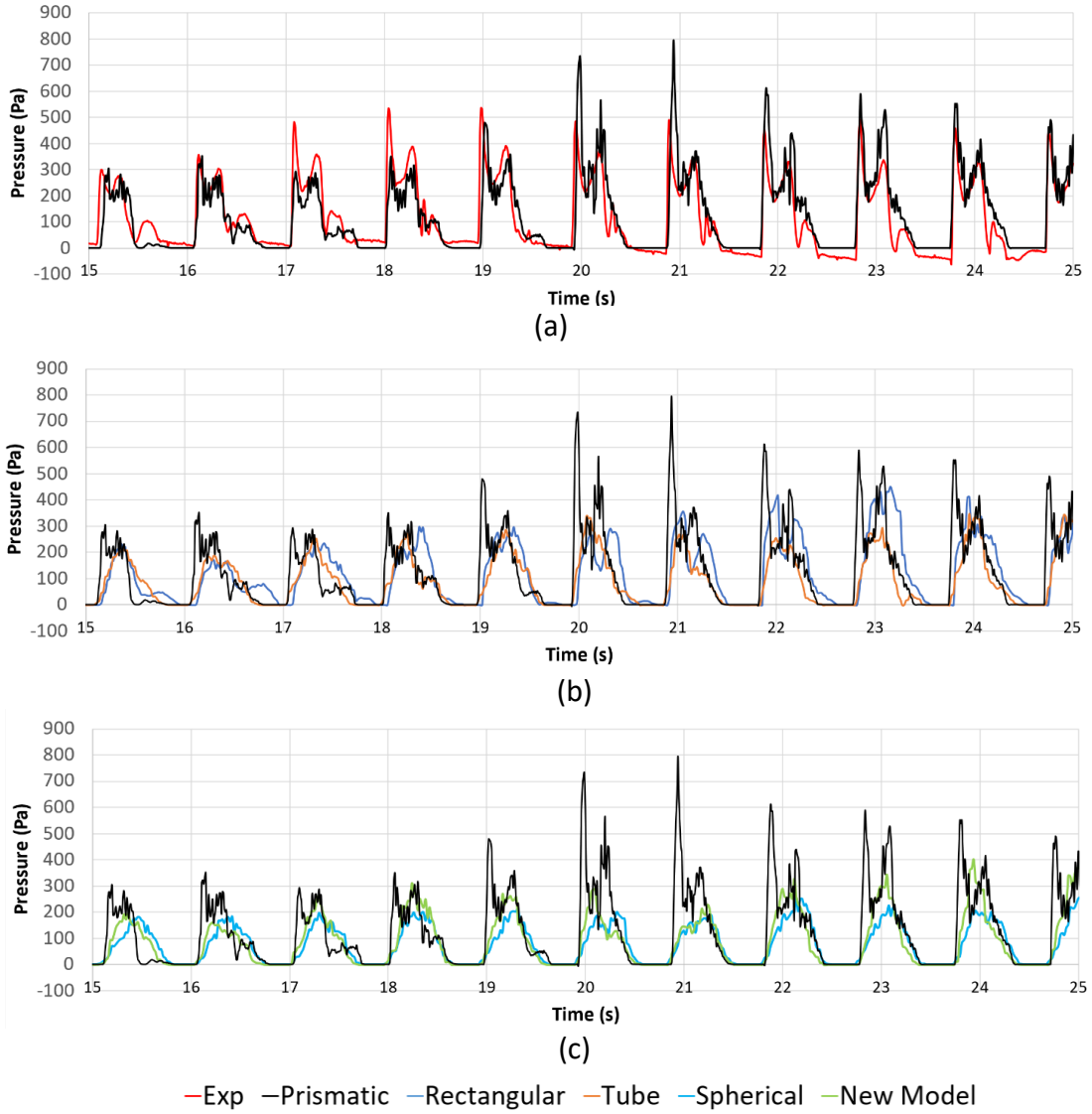

Fig. 6. Comparison of dynamic pressure for (a) SPH and experiment prismatic, (b) rectangular, tube, and (c) spherical, the new model in 25% filling ratio

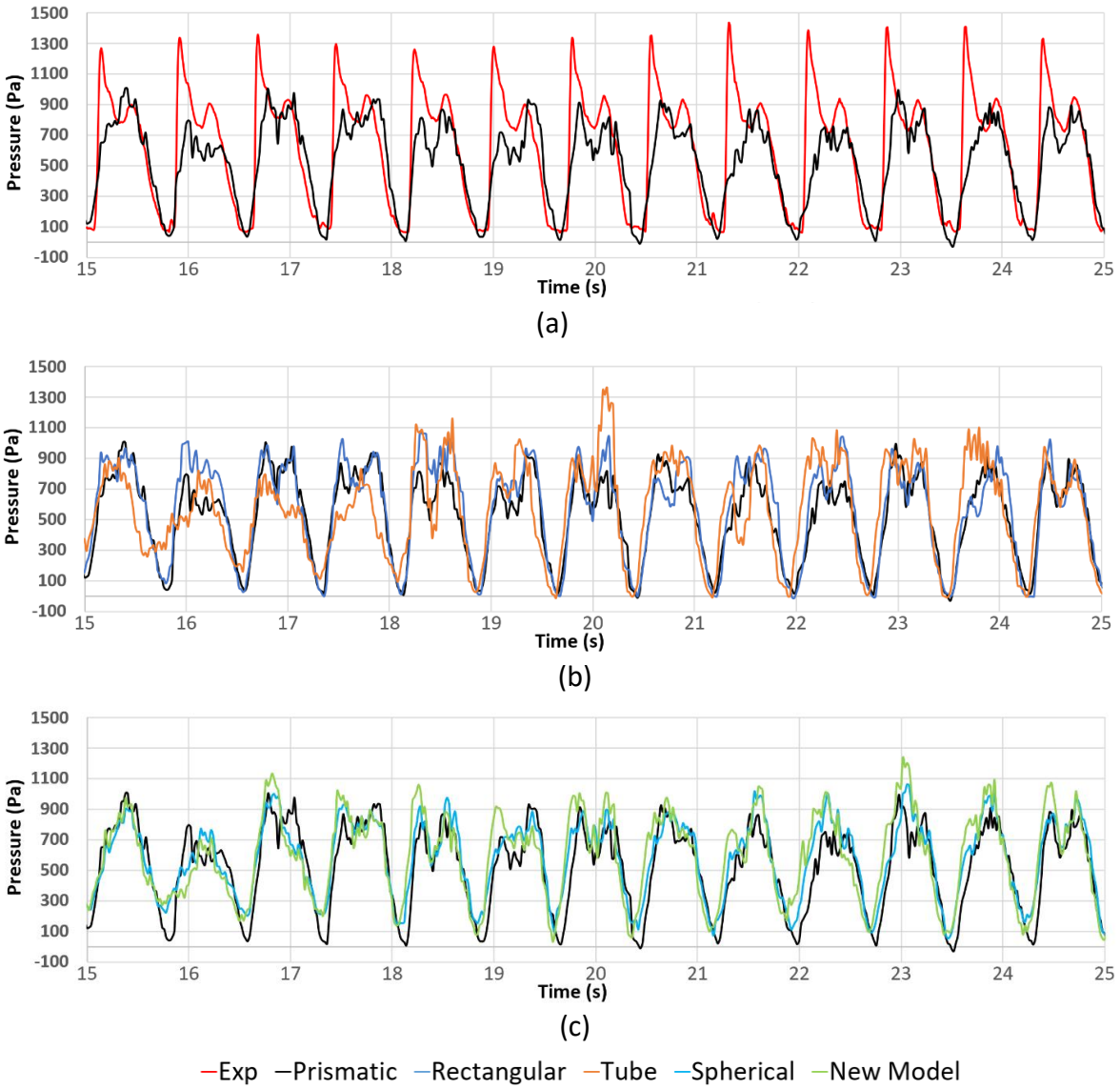

Fig. 7. Comparison of dynamic pressure for SPH and experiment prismatic (a) and with rectangular, tube (b), and spherical, new model (c) in 50% filling ratio

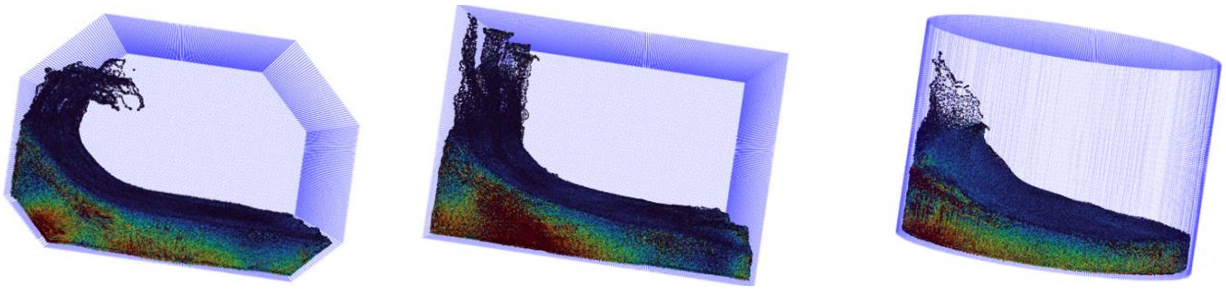

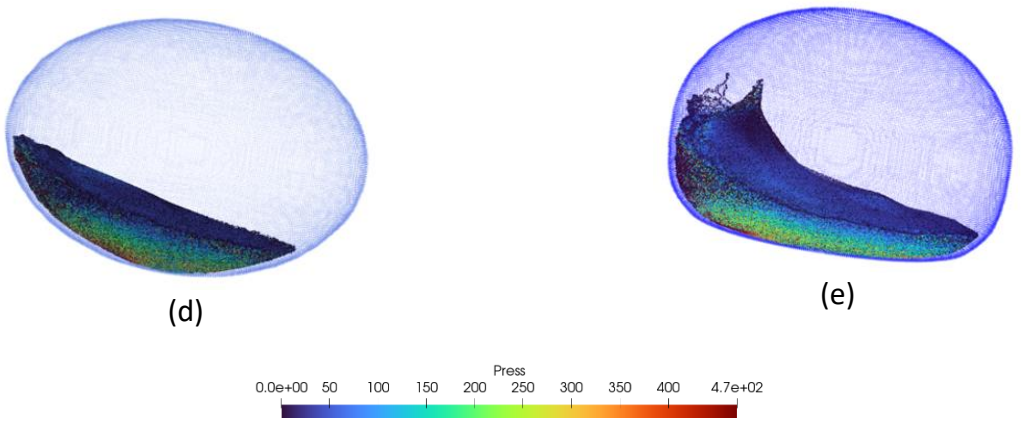

Fig. 8. Pressure contour of dynamic pressure (a) prismatic tank, (b) rectangular tank, (c) tube tank, (d) spherical tank, and (e) new model tank in 25% filling ratio

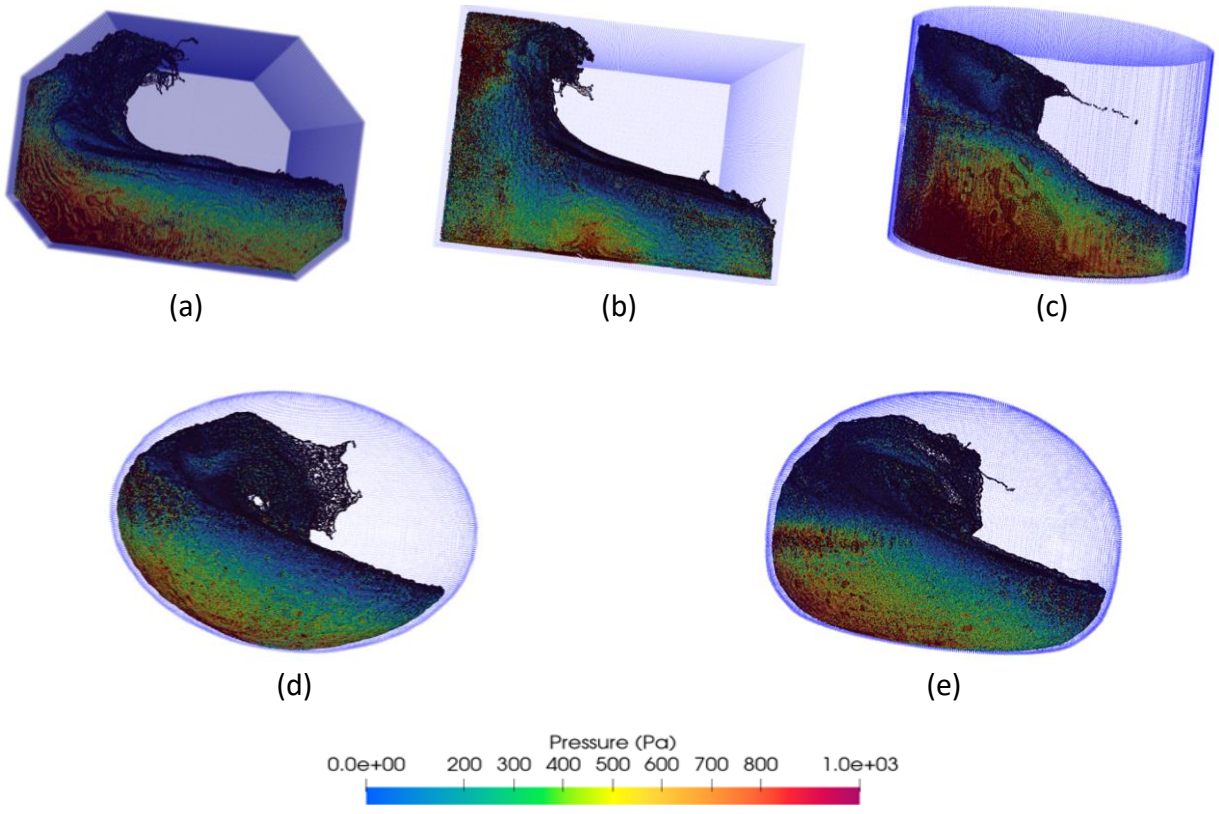

Fig. 9. Pressure contour of dynamic pressure (a) prismatic tank, (b) rectangular tank, (c) tube tank, (d) spherical tank, and (e) new model tank in 50% filling ratio

3.2 Free Surface Deformation

Figure 10 shows the snapshot of free surface deformation in the leading position in the sloshing simulation in the velocity vector. It shows that each tank shapes give differently damped fluid movement. Although sloshing is moderate in this situation, the tube and new model tank could reduce the wave created by sloshing flow. The fluid looked like in the rest condition; as a result, the dynamic pressure was decreased, as shown in Figure 8 and Figure 9. The free surface deformation of sloshing in the prismatic, rectangular, tube, spherical and new model tanks was carried out Using

Blender 2.92 for improved visualization. Advanced post-processing visualization has become more accessible thanks to VisualSPHysics; fluid becomes more attractive texturing than iso-surface or particle form. Figure 11. illustrates the vector velocity for sloshing on the five simulated tank shapes with a 25% and 50% filling ratio. It can be seen that waves are created after fluid is forced to move in the opposite wall. Compared to the prismatic tank with the other four tank shapes, velocities are reduced because the fluid conjoined in the middle of the tank with curved walls velocities decreased, as seen in Figure 10. There is vorticity because the fluid crashes the walls and spreads after passing the wall, which results in the fluid velocities decreasing and fluid becoming slower. It indicates that tubes and new-model tanks effectively reduce the movement of fluid. The tube and new model tank are reduced velocities due to the crashing fluid spreading on the wall near the free surface and the damped wave. Figure 11 illustrates free surface deformation in the prismatic, rectangular, tube, spherical and new model tanks using VisualSPHysics. The fluid is more pleasant when generated using VisualSPHysics. Compared to mesh based CFD, the results are one of the most advanced particle approaches. Further work will need to be carried out for two-phase SPH in a 3D model to see the effect of the mixture of air and water.

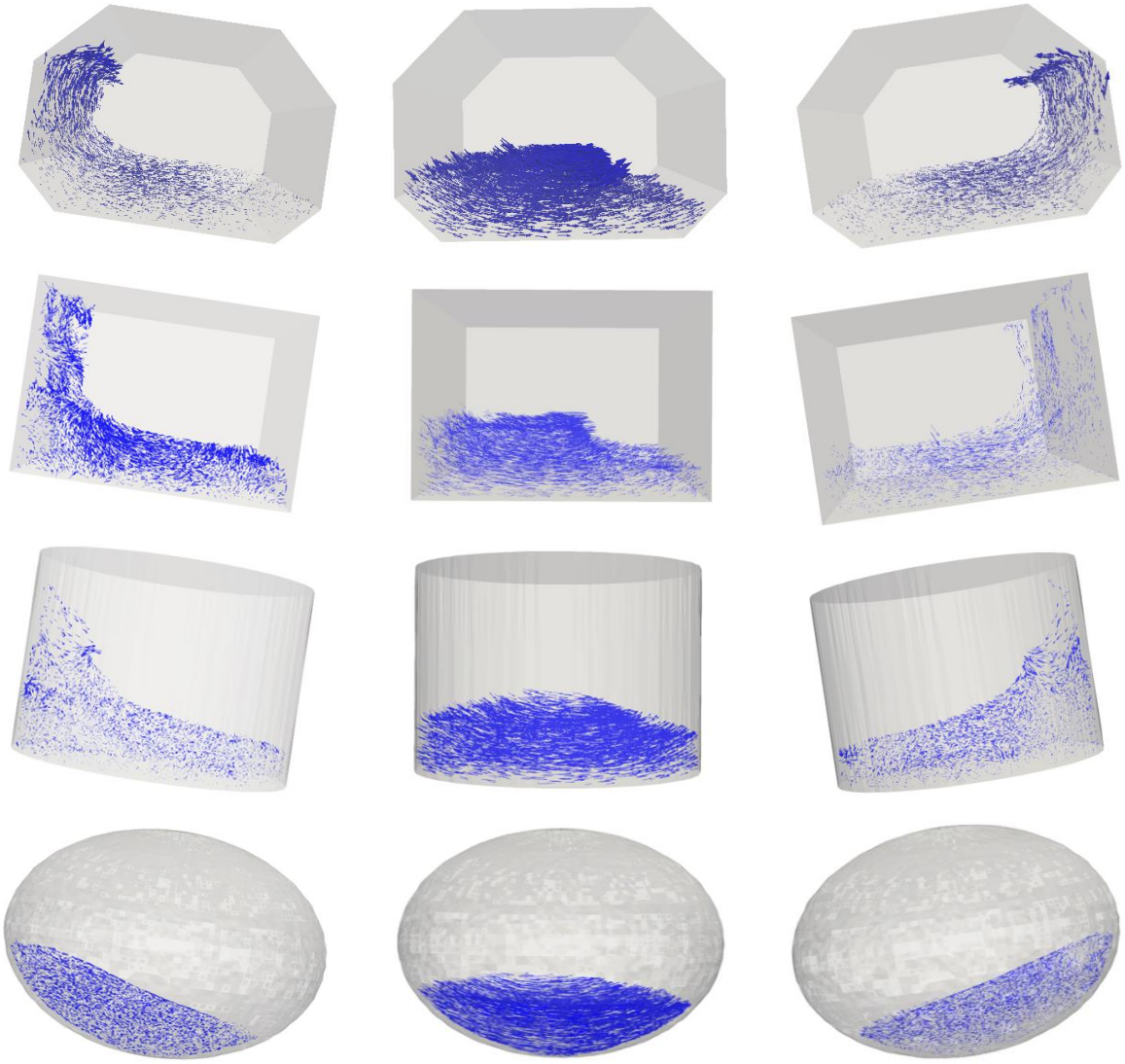

Fig. 10. Comparison of vector velocity inside prismatic, rectangular, tube, spherical and new model tanks in the filling ratio (a) 25% and (b) 50%

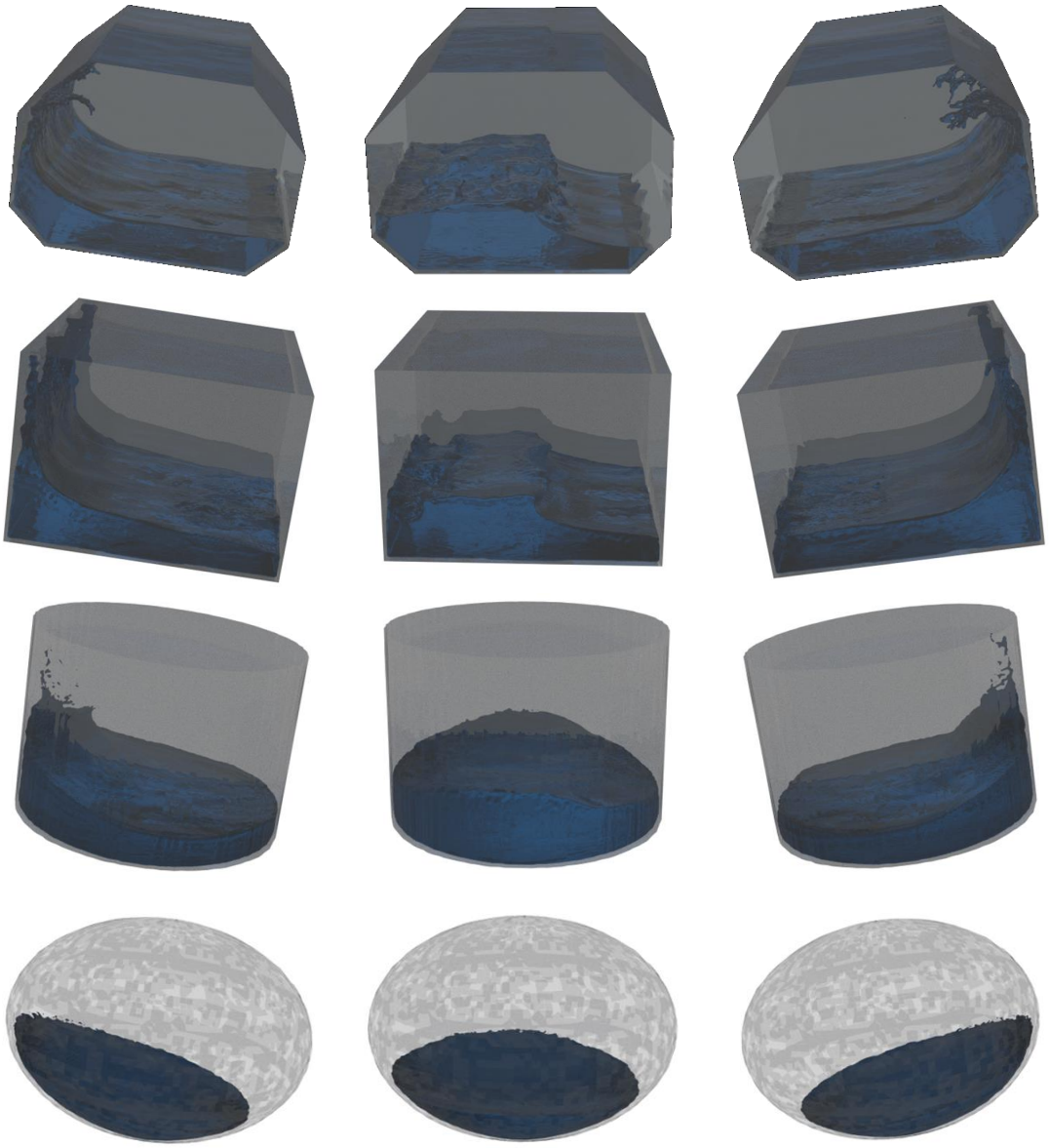

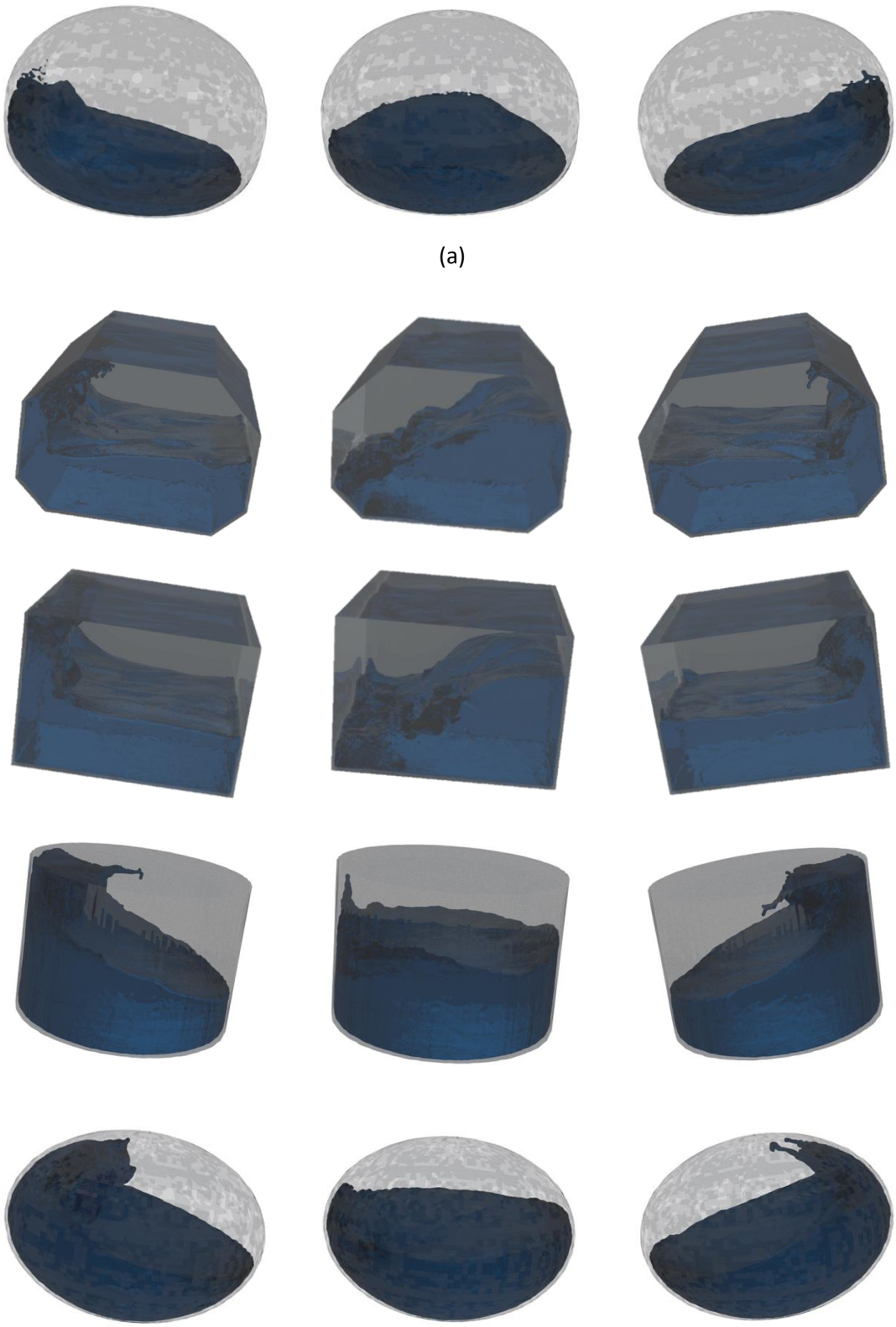

(a)

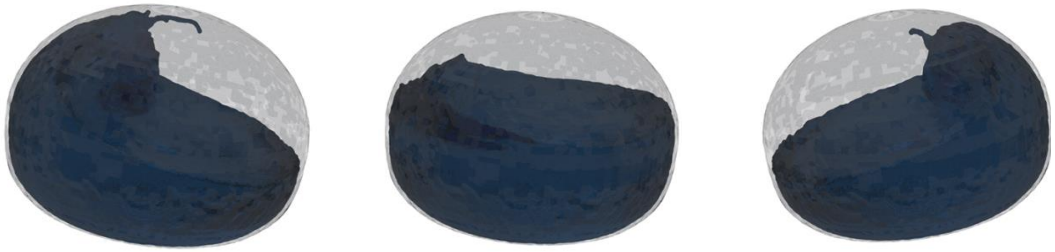

(b)

Fig. 11. Comparison of free surface deformation inside prismatic, rectangular, tube, spherical and new model tanks in the filling ratio 25% (a) and 50% (b)

3.3 Hydrodynamic Force

This section's findings discuss the hydrodynamic force of sloshing in the prismatic, rectangular, tube, spherical and new model tanks. The fluid inside the tank was made to move by an oscillation mechanism, and as a result, hydrodynamic force exists. Figure 12 compares the hydrodynamic force with 25% and 50% filling ratios; the black, orange, red, yellow, and blue lines represent prismatic, rectangular, tube, spherical, and new model tanks, respectively. The hydrodynamic force is greater on the rectangular tank than on the other. Figure 12 shows that the value of the hydrodynamics force on the tube and new model tanks is reduced by 40% at a 25% filling ratio and a 30% reduction at a 50% filling ratio compared to a prismatic tank. Thus, different tank shapes, namely tubes and new models, can be an alternative to reduce sloshing in vessels carrying liquid.

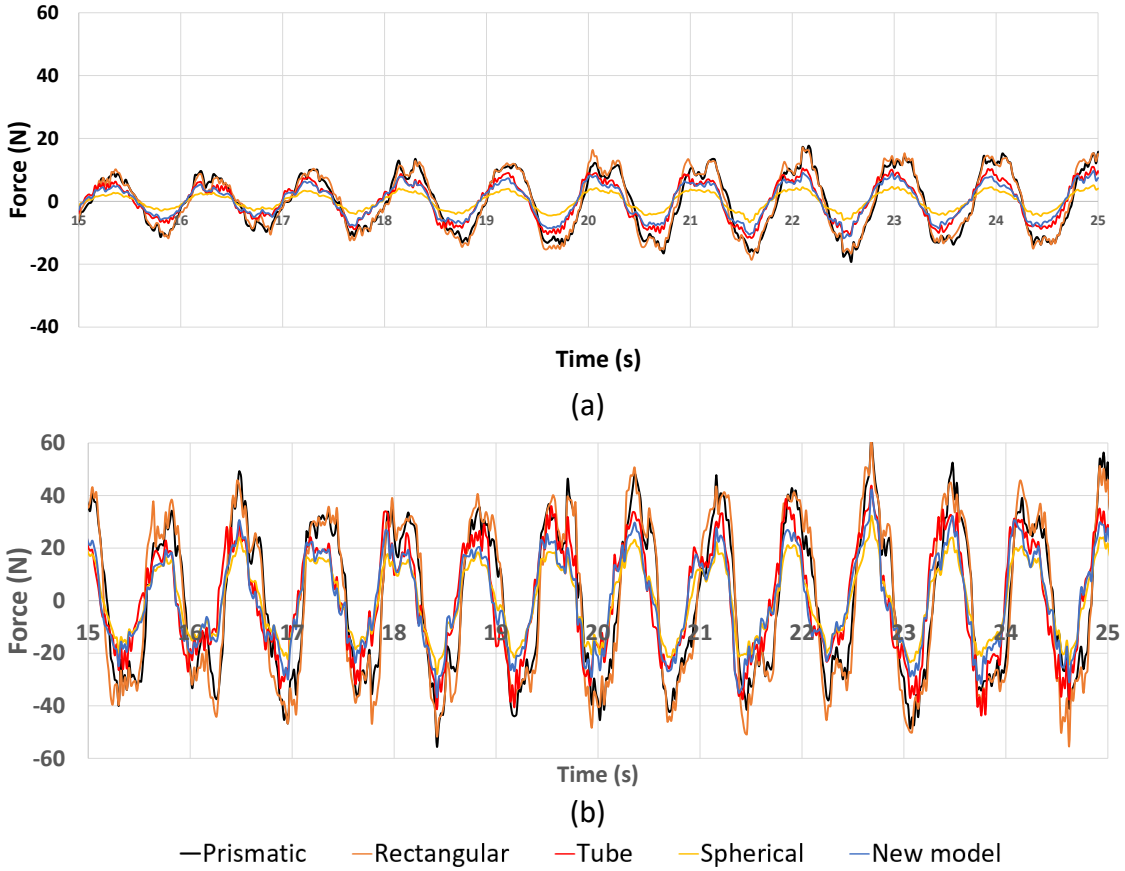

Fig. 12. The hydrodynamic force for 25% filling ratio (a) and 50% filling ratio (b)

4. Conclusions

It showed SPH successfully reproduced the sloshing phenomenon in different tank shapes, with same filling ratios and water depth. The result illustrates a difference of 9% for the tube tank and 11% for the new model tank for a filling ratio of 25%. In the filling ratio of 50%, there is a minor difference between the tube and the new model tank; it showed that the shape of the tank has minor dynamic pressure and hydrodynamic force. The findings indicate that tube and new model tanks are more effective at reducing sloshing than rectangular and spherical tanks. Additionally, they successfully reduced the dynamic pressure produced by energetic sloshing. Like the dynamic pressure phenomenon, these tank shapes successfully lowered the hydrodynamic force.

A sophisticated post-processing method employing VisualSPHysics was also used to obtain realistic fluid visualization. It was demonstrated that SPH might be applied to both scientific research and other objectives, including entertainment and industrial applications. Nonetheless, future research of two-phase SPH for three dimensions of prismatic, rectangular, tube, spherical and new model tanks need to carry out.

Acknowledgement

This research was funded by the Institute for Research and community services Diponegoro University (LPPM UNDIP) under the scheme international publication grant (RPI), grant number 225-39/UN7.D2/PP/IV/2023.

References

[1] Monaghan, J.J. “Simulating Free Surface Flows with SPH.” *Journal of Computational Physics* 110, no. 2 (1994): 399–406. https://doi.org/10.1006/jcph.1994.1034

[2] Monaghan, J.J., and A. Kocharyan. “SPH Simulation of Multi-Phase Flow.” *Computer Physics Communications* 87, no. 1–2 (May 2, 1995): 225–35. https://doi.org/10.1016/0010-4655(94)00174-Z

[3] Green, Mashy D., and Joaquim Peiró. “Long Duration SPH Simulations of Sloshing in Tanks with a Low Fill Ratio and High Stretching.” *Computers & Fluids* 174 (September 16, 2018): 179–99. https://doi.org/10.1016/j.compfluid.2018.07.006

[4] Green, Mashy D., Yipeng Zhou, José M. Dominguez, Moncho G. Gesteira, and Joaquim Peiró. “Smooth Particle Hydrodynamics Simulations of Long-Duration Violent Three-Dimensional Sloshing in Tanks.” *Ocean Engineering* 229 (2021): 108925. https://doi.org/10.1016/j.oceaneng.2021.108925

[5] Pilloton, C, A Bardazzi, A Colagrossi, and S Marrone. “SPH Method for Long-Time Simulations of Sloshing Flows in LNG Tanks.” *European Journal of Mechanics - B/Fluids* 93 (2022): 65–92. https://doi.org/https://doi.org/10.1016/j.euromechflu.2022.01.002

[6] Yang, Xi, Zhifan Zhang, Guiyong Zhang, Song Feng, and Zhe Sun. “Simulating Multi-Phase Sloshing Flows with the SPH Method.” *Applied Ocean Research* 118 (2022): 102989. https://doi.org/https://doi.org/10.1016/j.apor.2021.102989

[7] Trimulyono, Andi, Samuel, and Muhammad Iqbal. “Sloshing Simulation of Single-Phase and Two-Phase SPH Using DualSPHysics.” *Kapal: Jurnal Ilmu Pengetahuan Dan Teknologi Kelautan* 17, no. 2 (2020): 50–57. https://doi.org/10.14710/kapal.v17i2.27892

[8] Trimulyono, A., D. Chrismianto, Samuel Samuel, and M. H. Aslami. “Single-Phase and Two-Phase Smoothed Particle Hydrodynamics for Sloshing in the Low Filling Ratio of the Prismatic Tank.” *International Journal of Engineering, Transactions B: Applications* 34, no. 5 (2021): 1345–51. https://doi.org/10.5829/ije.2021.34.05b.30

[9] Ren, Yaru, Abbas Khayyer, Pengzhi Lin, and Xiangyu Hu. “Numerical Modeling of Sloshing Flow Interaction with an Elastic Baffle Using SPHinXsys.” *Ocean Engineering* 267 (2023): 113110. https://doi.org/10.1016/j.oceaneng.2022.113110

[10] Trimulyono, Andi, Atthariq Haikal, Chrismianto Deddy, and Samuel Samuel. “Investigation of Sloshing in The Prismatic Tank With Vertical And T-Shape Baffles.” *Brodogradnja* 73, no. 2 (2022): 43–58. https://doi.org/10.21278/brod73203

[11] Trimulyono, Andi, Deddy Chrismianto, Haikal Atthariq, and Samuel. "Numerical Simulation Low Filling Ratio of Sway Sloshing in the Prismatic Tank Using Smoothed Particle Hydrodynamics." *CFD Letters* 14, no. 7 (2022): 113–23. https://doi.org/10.37934/cfdl.14.7.113123

[12] Liu, Zhan, Hong Chen, Qiang Chen, and Liubiao Chen. "Numerical Study on Thermodynamic Performance in a Cryogenic Fuel Storage Tank Under External Sloshing Excitation." International Journal of Aeronautical and Space Sciences 22, no. 5 (2021): 1062–74. https://doi.org/10.1007/s42405-021-00385-9

[13] Liu, Zhan, Kaifeng Yuan, Yuanliang Liu, Martin Andersson, and Yanzhong Li. "Fluid Sloshing Hydrodynamics in a Cryogenic Fuel Storage Tank under Different Order Natural Frequencies." Journal of Energy Storage 52, no. PA (2022): 104830. https://doi.org/10.1016/j.est.2022.104830

[14] Liu, Zhan, Kaifeng Yuan, Yuanliang Liu, Yinan Qiu, and Gang Lei. "Fluid Sloshing Thermo-Mechanical Characteristic in a Cryogenic Fuel Storage Tank under Different Gravity Acceleration Levels." International Journal of Hydrogen Energy 47, no. 59 (2022): 25007–21. https://doi.org/10.1016/j.ijhydene.2022.05.243

[15] Subramaniam, Thineshwaran, and Mohammad Rasidi Rasani. "Pulsatile CFD Numerical Simulation to Investigate the Effect of Various Degree and Position of Stenosis on Carotid Artery Hemodynamics." *Journal of Advanced Research in Applied Sciences and Engineering Technology* 26, no. 2 (2022): 29–40. https://doi.org/10.37934/araset.26.2.2940

[16] Noh, Arina Mohd, Sohif Mat, and Mohd Hafidz Ruslan. "CFD Simulation of Temperature and Air Flow Distribution inside Industrial Scale Solar Dryer." *Journal of Advanced Research in Fluid Mechanics and Thermal Sciences* 45, no. 1 (2018): 156–64.

[17] Adanta, Dendy, Mochammad Malik Ibrahim, Dewi Puspita Sari, Imam Syofii, and Muhammad Amsal Ade Saputra. "Application of the Grid Convergency Index Method and Courant Number Analysis for Propeller Turbine Simulation." *Journal of Advanced Research in Fluid Mechanics and Thermal Sciences* 96, no. 2 (2022): 33–41. https://doi.org/10.37934/arfmts.96.2.3341

[18] Musa, Solihin, Nor Azwadi Che Sidik, Siti Nurul Akmal Yusof, Teknologi Malaysia, Jalan Sultan Yahya Petra, and Kuala Lumpur. "Analysis of Internal Flow in Bag Filter by Different Inlet Angle." *Journal of Advanced Research in Numerical Heat Transfer* 3, no. 1 (2020): 12–24. https://www.akademiabaru.com/submit/index.php/arnht/article/view/1365

[19] Trimulyono, Andi, Hirotada Hashimoto, and Akihiko Matsuda. "Experimental Validation of Single- and Two-Phase Smoothed Particle Hydrodynamics on Sloshing in a Prismatic Tank." *Journal of Marine Science and Engineering* 7, no. 8 (2019). https://doi.org/10.3390/jmse7080247

[20] Domínguez, J M, G Fourtakas, C Altomare, R B Canelas, A Tafuni, O García-Feal, I Martínez-Estévez, et al. "DualSPHysics: From Fluid Dynamics to Multiphysics Problems." *Computational Particle Mechanics* 9, no. 5 (2022): 867–95. https://doi.org/10.1007/s40571-021-00404-2

[21] Crespo, A.J.C., J.M. Domínguez, B.D. Rogers, M. Gómez-Gesteira, S. Longshaw, R. Canelas, R. Vacondio, A. Barreiro, and O. García-Feal. "DualSPHysics: Open-Source Parallel CFD Solver Based on Smoothed Particle Hydrodynamics (SPH)." *Computer Physics Communications* 187 (2015): 204–16. https://doi.org/10.1016/j.cpc.2014.10.00

[22] García-Feal, O, A J C Crespo, and M Gómez-Gesteira. "VisualSPHysics: Advanced Fluid Visualization for SPH Models." *Computational Particle Mechanics* 9, no. 5 (2022): 897–910. https://doi.org/10.1007/s40571-020-00386-7

[23] Liu, G. R, Liu MB. Smoothed Particle Hydrodynamics: A Meshfree Particle Method. World Scientific Publishing Company; 2003. https://doi.org/10.1142/9789812564405

[24] Molteni D, Colagrossi A. A simple procedure to improve the pressure evaluation in hydrodynamic context using the SPH. Comput Phys Commun 2009;180:861–72. https://doi.org/10.1016/j.cpc.2008.12.004

[25] Crespo AJC, Gomez-Gesteira M, Dalrymple RA. Boundary Conditions Generated by Dynamic Particles in SPH Methods. Comput Mater Contin 2007;5:173–84

[26] English A, Domínguez JM, Vacondio R, Crespo AJC, Stansby PK, Lind SJ, et al. Modified dynamic boundary conditions (mDBC) for general-purpose smoothed particle hydrodynamics (SPH): application to tank sloshing, dam break and fish pass problems. Comput Part Mech 2022;9:1–15. https://doi.org/10.1007/s40571-021-00403-3